Automatica 142 (2022) 110350

Contents lists available at ScienceDirect

Automatica

journal homepage: www.elsevier.com/locate/automatica

Brief paper

Interpretable fault diagnosis with shapelet temporal logic: Theory and application☆

Gang Chen [a,*], Yu Lu [b], Rong Su [c]

[a] Shien-Ming Wu School of Intelligent Engineering, South China University of Technology, 511442, Guangzhou, China
[b] School of Energy and Power Engineering, Nanjing University of Science and Technology, 210094, Nanjing, China
[c] School of Electrical and Electronic Engineering, Nanyang Technological University, 50 Nanyang Avenue, Singapore, 639798, Singapore

ARTICLE INFO

Article history:
Received 30 March 2021
Received in revised form 21 December 2021
Accepted 11 March 2022
Available online xxxx

Keywords:
Interpretable fault diagnosis
Logic inference
Monotonic order
Rolling element bearing
Shapelet temporal logic

ABSTRACT

Shapelets are discriminative subsequences of sequential data that best predict the target variable and are directly interpretable, which have attracted considerable interest within the interpretable fault diagnosis community. Despite their immense potential as a data mining primitive, currently, shapelet-based methods ignore the temporal properties of shapelets. This paper presents a shapelet temporal logic, which is an expressive formal language to describe the temporal properties of shapelets. Moreover, an incremental algorithm is proposed to find the optimal logic expression with formal and theoretical guarantees, and the obtained logic expression can be used for fault diagnosis. Additionally, a case study on rolling element bearing fault diagnosis shows the proposed method can diagnose and interpret faults with high accuracy. Comparison experiments with other logic-based and shapelet-based methods illustrate the proposed method has better interpretability at the cost of computation efficiency.

© 2022 Elsevier Ltd. All rights reserved.

1. Introduction

Fault diagnosis methods based on time series classification (TSC) diagnose fault by classifying the fault types. However, traditional fault classification methods cannot provide further interpretations for better fault maintenance. Many scholars have tried to propose interpretable TSC methods to equip the fault diagnosis results with interpretability (Zhao et al., 2021). Interpretability means understanding the decision process of fault diagnosis. However, until now, there is neither complete theory and method of pure mathematical analysis nor formal mathematical definition for interpretability (Yang et al., 2020). To approach interpretable fault diagnosis results, most existing works pay attention to using visualization to connect the key features to the decision and providing a visual and empirical explanation for users. The goal of interpretation is to make users feel the results of the decision are in line with our understanding about the physical process. However, the interpretation is empirical and not formal, where the users need many numerical experiments and much background knowledge to approach an interpretation of the results.

Shapelets, which were introduced in 2009 as a primitive for time series classification in Ye and Keogh (2009), have attracted a lot of attention in interpretable time series classification (Bergé et al., 2019). Shapelets are time series subsequences that are representative of class membership. The idea is that different classes of time series can often exhibit inter-class differences in terms of small subsequences rather than the full series structure. Therefore, shapelets identify short discriminative series segments (Ye & Keogh, 2009). Time series classification with shapelets offers several benefits over competing approaches. Firstly, shapelets can indicate the inherent structure of the data in a manner that is directly interpretable and can offer intuitive insights into the problem domain. Secondly, shapelet classifiers are more compact than many other methods. We only need a small number of shapelets (sometimes only one) for classification tasks, instead of comparison to the entire dataset. Thirdly, shapelets are sensitive to the phase-independent shape-based similarity of subsequences, which is hard to detect for algorithms based on the whole series. Despite the aforementioned promising features of shapelets for fault diagnosis, there are also two important limitations of shapelets. Firstly, their expressiveness is limited to simple binary presence/absence questions (Mueen et al., 2011). Thus, the logical-shapelets were proposed, which allows the combination of multiply shapelets with conjunction and disjunction

☆ This research is supported by the Agency for Science, Technology and Research (A*STAR) under its IAF-ICP Programme ICP1900093 and the Schaeffler Hub for Advanced Research at NTU. The material in this paper was not presented at any conference. This paper was recommended for publication in revised form by Associate Editor Angelo Alessandri under the direction of Editor Thomas Parisini.

* Corresponding author.
E-mail addresses: gangchen@scut.edu.cn (G. Chen), yu.lu@njust.edu.cn (Y. Lu), rsu@ntu.edu.sg (R. Su).

https://doi.org/10.1016/j.automatica.2022.110350
0005-1098/© 2022 Elsevier Ltd. All rights reserved.

operators, to enrich the complexity of the patterns that shapelets can express in Mueen et al. (2011). However, logical-shapelets ignore the temporal relationship between shapelets, and it is also limited to binary questions. Secondly, the time taken to compute shapelets is significant (Baldán & Benítez, 2019). When shapelets were first proposed, all possible subsequences were considered as potential candidates, while the minimum distances of a candidate to all training series were used as a predictor feature for ranking the quality of the subsequences. A detailed description of efficient shapelet methods can be found in Baldán and Benítez (2019) and omitted here due to page limit.

In this paper, inspired by another interpretable time series classification primitive, called signal temporal logic (STL) (Deshmukh et al., 2017), which is an expressive specification language used in the field of formal methods to specify behaviors of continuous systems, we take the shapelets into a temporal logic definition and address the expensiveness problem of traditional shapelets by defining a new formal language, called shapelet temporal logic (ShTL). ShTL is equipped with the capacity to describe the temporal relationship among shapelets. ShTL not only has the time-invariance property of shapelets, but also can describe the shifted variance pattern of time series. Moreover, the quantitative semantics of ShTL can tell how much a given time series satisfies the shapelet properties, not limited to only binary questions. Additionally, the distance metrics for two shapelets do not depend only on the upper and lower bounds of the time series as STL, which is more robust to noise compared with STL. To address the time consuming logic inference problem, we introduce two novel techniques to speed up the search for the ShTL-based logic description for time series. Firstly, we derive some lemmas and theorems about the properties of ShTL. Based on these theoretical results, we transform the logic inference problem into a sequence of optimization problems, using the properties of the formal language to guide the search. Secondly, we choose the best k shapelets and precompute the distance between time series and shapelets, i.e., we do not need to compute the distance during the logic inference process. In essence, we trade time for space, such that with a small relativity increase in the space required, we have significantly reduced the time required (see Section 5.1 for detail). It is important to note that there is essentially zero-cost for the expressiveness of ShTL. In other words, if we apply them to a dataset that does not need their increased representational power, they will have a similar property with classic shapelets, where the bounded time is equivalent to the whole time series. Therefore, the proposed work complements and further enables the growing interest in shapelets as an interpretable data mining tool.

2. Definition and background

A time series $\mathbf{x}$ is a sequence of real numbers $x_1, x_2, \ldots, x_m \in \mathbb{R}$, sampled at equal time intervals. We use $\mathbf{x}[i]$ to denote x_i.

Definition 1 (*Shapelet*)**.** A shapelet $\mathbf{x}[i, l] = x_i, x_{i+1}, \ldots, x_{i+l-1}$ is a continuous subsequence of time series $\mathbf{x}$ starting at position i with length l.

Based on the definition of shapelets, a time series of length m can have $m(m+1)/2$ shapelets of all possible lengths from 1 to m. Time series classification based on shapelets mainly relies on the chosen distance or similarity metrics to discriminate two shapelets. The distance metric defines the distance function $d(\cdot)$ that compares two time series of equal length. Then, classification can be performed by identifying the closest subsequence match in the target time series. Since tiny differences in scale and offset rapidly swamp any similarity in shape (Keogh & Kasetty, 2003), to achieve scale and offset invariance, the *z-normalization* is applied to the individual time series before the actual distance is computed. Various distance metrics have been used, depending on the application scenarios and properties of the time series. Here we define the time-varying distance metrics shown as follows.

$$f(s, \mathbf{x}, i) = d(s, \mathbf{x}[i, l]), \tag{1}$$

where $i \leq m - l + 1$, and the distance metrics $d(\cdot, \cdot)$ used in this paper is the normalized Euclidean distance.

2.1. Shapelet temporal logic

Definition 2 (*Shapelet Temporal Logic*)**.** Given a shapelet s and a time series $\mathbf{x}$. *Shapelet temporal logic* (ShTL) is a temporal logic defined over time series shapelet distance. ShTL is a predicate logic with interval-based temporal semantics. The syntax of ShTL is defined recursively as,

$$\varphi := \mu | \neg\varphi | \varphi_1 \vee \varphi_2 | \varphi_1 \wedge \varphi_2 | F_{[a,b)}\varphi | G_{[a,b)}\varphi, \tag{2}$$

where a and b are non-negative finite real numbers, and $\mu = f(s, \mathbf{x}, i) \leq \gamma$ is a predicate, where $f(s, \mathbf{x}, i)$ is defined in Eq. (1), and $\gamma \in \mathbb{R}^+$ is a constant. The Boolean operators $\neg$, $\vee$ and $\wedge$ are negation ("not"), disjunction ("or") and conjunction ("and"), respectively. The temporal operators F and G stand for "Finally (eventually)" and "Globally (always)", respectively.

Remark 1. The syntax of ShTL is similar with STL in Chen et al. (2020). But the distance metric for STL is defined as the distance between the signal and a predefined value among a time interval, which is sensitive to the predefined value and noise, i.e., a noise will change the distance easily. However, the distance metric for ShTL is the normalized Euclidean distance between a piece of signal and the shapelet, in which the noise's effect will be averaged among the shapelet, thus more robust to noise. This transformation releases the noisy sensitivity property of STL. Moreover, any distance or similarity measure can be employed as the distance metric. Similar to signal temporal logic (Chen et al., 2020), ShTL is also equipped with quantitative semantics. The quantitative semantics, call *robustness degree* (also called "degree of satisfaction") that quantifies how well a given time series $\mathbf{x}$ satisfies a given formula φ_s with respect to shapelet s at time i, denoted as $\rho(\mathbf{x}, \varphi, i)$ which can be defined similarly with STL as in Chen et al. (2020).

The robustness degree is sound, meaning that $\rho(\mathbf{x}, \varphi, i) \geq 0$ implies that time series $\mathbf{x}$ satisfies φ at time i, denoted as $\mathbf{x}[i, l] \models_s \varphi$, and $\rho(\mathbf{x}, \varphi, i) < 0$ implies that time series $\mathbf{x}$ violates φ at time i, denoted as $\mathbf{x}[i, l] \not\models_s \varphi$. Therefore, to check whether a time series $\mathbf{x}$ satisfies a formula φ at i, we only need to calculate the robustness degree $\rho(\mathbf{x}, \varphi, i)$. In the rest of this paper, we denote the robustness degree of formula φ at time 0 with respect to time series $\mathbf{x}$ by $\rho(\mathbf{x}, \varphi)$ for short. If $\rho(\mathbf{x}, \varphi)$ is large and positive, then $\mathbf{x}$ would have to deviate substantially in order to violate φ. The above definition also indicates that robustness degree $\rho(\mathbf{x}, \varphi)$ depends on some pieces of $\mathbf{x}$, not all series of $\mathbf{x}$, we call the intervals that expanded by the pieces as *effective interval* of a formula φ with respect to $\mathbf{x}$. ShTL can be extended to *Parametric shapelet temporal logic (pShTL)*, where the bound γ and the endpoints of the time intervals $[a, b)$ are parameters instead of constants. For example, if $\varphi_\theta = F_{[\tau_1,\tau_2)}(f(s, \mathbf{x}, i) \leq \pi_1)$ with parameter vector $\theta = [\pi_1, \tau_1, \tau_2]$, then $\varphi_\theta = F_{[0,3)}(f(s, \mathbf{x}, i) < 0)$.

In the following, we will use φ_{θ_i} (or φ_{θ^*}) to denote the ShTL formula resulting from valuating the parameters θ of the pShTL formula φ_θ. With pShTL, we can define the extended language of a formula φ with respect to shapelet s as

$$\mathcal{L}^e(\varphi) = \left\{\mathbf{x} | \mathbf{x} \in \mathcal{L}(\varphi_\theta), \forall\theta \in \mathbb{R}^n\right\}, \tag{3}$$

where n is the dimension of the parameter vector.

ShTL is an expressive formal language and can be used to describe a wide range of time series properties, such as (1) Bounded-time invariance, e.g., $F_{[0,a)}G_{[b,c)}(f(s,\mathbf{x},i) \leq \pi)$ denotes "there exists a time $i \in [0,a)$, such that $f(s,\mathbf{x},i) \leq \pi$ will be hold in $[i+b, i+c)$"; (2) Cyclical shapelets, e.g., $G_{[0,a)}F_{[0,b)}(f(s,\mathbf{x},i) \leq 0.1)$ denotes "$f(s,\mathbf{x},i) \leq 0.1$ (shapelet s) will be hold within every time interval $[i, i+b)$ for all $i \in [0,a)$"; (3) Multiple shapelets coupling, e.g., $F_{[0,a)}(f(s,\mathbf{x},i) \leq \pi_1) \wedge F_{[0,b)}(f(s',\mathbf{x},i) \leq \pi_2)$ denotes "there exists a time $i \in [0,a)$, such that eventually $f(s,\mathbf{x},i)$ will be not larger than π_1 and there exists a time $i \in [0,b)$, such that eventually $f(s',\mathbf{x},i)$ is not larger than π_2", where s and s' are two shapelets.

3. Problem formulation

Now we formally define the problem solved in this paper.

Problem 1. Given a set of time series $\Gamma = \Upsilon^+ \cup \Upsilon^-$, where Υ^+, indicating the set of time series that have desirable behaviors, and Υ^-, indicating the set of time series that have undesirable behaviors, respectively, find a pShTL formula φ_D describing desirable behaviors (with subscript D indicates "desirable" behavior), such that the misclassification rate,

$$\epsilon(\Gamma, \varphi_D) = (FA + MD)/(|\Upsilon^+| + |\Upsilon^-|) \tag{4}$$

is minimized, where $|\cdot|$ denotes the cardinality of a set, $FA = |\{\mathbf{x}|\mathbf{x} \not\models_s \varphi_D, \mathbf{x} \in \Upsilon^+\}|$ is the number of false alarms (time series improperly classified) and $MD = |\{\mathbf{x}|\mathbf{x} \models_s \varphi_D, \mathbf{x} \in \Upsilon^-\}|$ is the number of missed detections (time series improperly classified as desirable).

This problem is a classical supervised learning problem, which is modified from the off-line anomaly learning problem defined in Chen et al. (2020). However, instead of using the original time series for classification, here we introduce shapelets and their distances of the original time series for logic formula learning. In the paper, the algorithm should make a decision to extend the pShTL formula and find the optimal parameters for the formula to optimize the misclassification rate.

4. Theoretical properties of pShTL

In this section, we derive some theoretical properties of pShTL that are important to solve the problem. The proofs of the theoretical results can be found in the Appendix.

Lemma 1. *Given pShTL formula $\varphi_1 = F_{[0,a)}\varphi$, $\varphi_2 = G_{[0,b)}\varphi$, and parameters a, b, c, the following statements hold: (1) if $\varphi_3 = F_{[0,c)}\varphi_1$, then $\mathcal{L}^e(\varphi_3) = \mathcal{L}^e(\varphi_1)$; (2) if $\varphi_3 = G_{[0,c)}\varphi_2$, then $\mathcal{L}^e(\varphi_3) = \mathcal{L}^e(\varphi_2)$; (3) if $\varphi_3 = G_{[0,c)}\varphi_1$, then $\mathcal{L}^e(\varphi_3) \subseteq \mathcal{L}^e(\varphi_1)$; (4) if $\varphi_3 = F_{[0,c)}\varphi_2$, then $\mathcal{L}^e(\varphi_2) \subseteq \mathcal{L}^e(\varphi_3)$.*

Lemma 1 shows that the expressiveness of some complex formulas with nesting temporal operators are equivalent to some simple formulas. Based on the results in Lemma 1, we have the following results.

Lemma 2. *For a pShTL formula $\varphi(\theta)$ with parameter vector θ, and for any time series $\mathbf{x}$, if $\mathbf{x} \models_s \varphi(\theta)$, then there exists a simpler form of φ with parameter vector θ', denoted as $\psi(\theta')$, such that $\mathbf{x} \models_s \psi(\theta')$, where ψ is simplified from φ by merging the nesting operator in φ and is defined recursively by syntax,*

$$\psi = \phi|\neg\phi|\phi_1 \wedge \phi_2|\phi_1 \vee \phi_2, \tag{5}$$

where $\phi \in \Omega$ is the atomic formula and $\Omega = \{(f(s,\mathbf{x},i) \leq \gamma), F_{[a,b)}(f(s,\mathbf{x},i) \leq \gamma), G_{[a,b)}(f(s,\mathbf{x},i) \leq \gamma), F_{[a,b)}G_{[c,d)}(f(s,\mathbf{x},i) \leq \gamma), G_{[a,b)}F_{[c,d)}(f(s,\mathbf{x},i) \leq \gamma), \neg\phi\}$.

The syntax in (5) is simpler and does not include temporal operators. Lemma 2 indicates that we can use some atomic formulas to construct pShTL formulas that have equivalent expressiveness with respect to pShTL formulas defined by the syntax in (2). This property allows us to omit the formulas that have complex nesting operators. Before we introduce the theorem of this paper, we define the concept of *effective interval* as follows.

Definition 3 (*Effective Interval*)**.** Given a set of time series T and an ShTL formula φ, if for all $\mathbf{x} \in T \Rightarrow \mathbf{x} \models_s \varphi$, then an effective interval is the shortest position interval, denoted as $\mathcal{E}(T,\varphi) = [m,n]$, such that for any time series $\mathbf{x} \in T$, the decision of $\mathbf{x} \models_s \varphi$ is based on $\mathbf{x}[m, n-m+1]$, namely other series of $\mathbf{x}$ do not affect the result of robustness calculation.

Definition 4 (*Parallel Formulas*)**.** Given a set of time series T, two ShTL formulas φ_1 and φ_2 are parallel formulas with respect to T, denoted as $\varphi_1 \parallel_T \varphi_2$, if for any series in T, the conjunction set of their effective intervals is empty.

The effective interval is defined over the same dimension. When the formulas are applied to different dimensions of the time series, they are always parallel formulas. Moreover, the effective interval is related to the temporal parameters of the formula, which captures the subsequence of time series that is related to decision making. To guide the search for an optimal formula, we define a relation denoted as $\preceq_s$, called *monotonic order*, for ShTL formulas as shown in Definition 5.

Definition 5 (*Monotonic Order*)**.** Given two labeled time series sets Υ^+ and Υ^-, indicating the set of desirable and undesirable behaviors, respectively, for two ShTL formulas φ_1 and φ_2, $\varphi_1 \preceq_s \varphi_2$ if the following conditions hold: (1) for all $\mathbf{x} \in \Upsilon^+$, $\mathbf{x} \models_s \varphi_1 \Rightarrow \mathbf{x} \models_s \varphi_2$; (2) for all $\mathbf{x} \in \Upsilon^-$, $\mathbf{x} \not\models_s \varphi_1 \Rightarrow \mathbf{x} \not\models_s \varphi_2$.

Lemma 3. *Given two labeled time series sets Υ^+ and Υ^-, indicating the set of time series that have desirable and undesirable behaviors, respectively, for two ShTL formulas φ_1, φ_2, and $\varphi_1 \parallel_T \varphi_2$, the following statements hold: (1) if for all $\mathbf{x} \in \Upsilon^+$, $\mathbf{x} \models_s \varphi_1$ and $\mathbf{x} \models_s \varphi_2$, implies $\varphi_1 \preceq_s \varphi_1 \wedge \varphi_2$; (2) if for all $\mathbf{x} \in \Upsilon^-$, $\mathbf{x} \not\models_s \varphi_1$ and $\mathbf{x} \not\models_s \varphi_2$, implies $\varphi_1 \preceq_s \varphi_1 \vee \varphi_2$.*

Based on the definition of parallel formula and monotonic order, the proof of Lemma 3 is trivial and omitted here. Accordingly, we have the following theorems.

Theorem 1. *Given two labeled time series sets Υ^+ and Υ^- as defined in Problem 1, if there exists an ShTL formula φ defined by syntax in Eq. (5), such that $\forall\mathbf{x} \in \Upsilon^+$, $\mathbf{x} \models_s \varphi$ and $\forall\mathbf{x} \in \Upsilon^-$, $\mathbf{x} \models_s \neg\varphi$, then there exists a sequence of pShTL formula $\varphi_1, \varphi_2, \ldots, \varphi_n$ with a proper parameter for each formula, such that $\varphi_1 \preceq_s \varphi_2, \ldots, \preceq_s \varphi_n \preceq_s \varphi$, $\varphi \preceq_s \varphi_n$ and $|\varphi_i| - |\varphi_{i-1}| = 1$, where $n \geq 1$ and $|\varphi_i|$ denotes the number of predicates in φ_i.*

Remark 2. Theorem 1 indicates that if there exists a pShTL formula can classify the time series, we can search for the formula through the monotonic order chain, which can start from a simple formula, then extends it based on monotonic order properties. Moreover, the monotonic properties indicate the search direction is to find the formula φ, which should: (1) be monotonic order with respect to the previous formula; (2) decrease the number of time series that belongs to Υ^- but satisfies φ. The following theorem shows that the searching can be started with any formula.

Theorem 2. *Given two labeled time series sets Υ^+ and Υ^- as defined in Problem 1, if there exists an ShTL formula φ, such that*

$\forall \mathbf{x} \in \Upsilon^+$, $\mathbf{x} \models_s \varphi$ *and* $\forall \mathbf{x} \in \Upsilon^-$, $\mathbf{x} \models_s \neg\varphi$, *then* $\forall \varphi_0$ *and* $\forall \mathbf{x} \in \Upsilon^+$, $\mathbf{x} \models_s \varphi_0$, *there exists a sequence of pShTL formula* $\varphi_1, \varphi_2, \ldots, \varphi_n$ *with proper parameters, such that* $\varphi_0 \preceq_s \varphi_1 \preceq_s \varphi_2, \ldots, \preceq_s \varphi_n \preceq_s \varphi$ *and* $\varphi \preceq_s \varphi_n$, *where* $n \geq 1$.

Corollary 1. *Given two labeled time series sets* Υ^+ *and* Υ^- *as defined in Problem 1, if there exists an ShTL formula* φ, *such that* $\forall \mathbf{x} \in \Upsilon^+$, $\mathbf{x} \models_s \varphi$ *and* $\forall \mathbf{x} \in \Upsilon^-$, $\mathbf{x} \models_s \neg\varphi$, *then* $\forall \varphi_0$ *and* $\forall \mathbf{x} \in \Upsilon^-$, $\mathbf{x} \models_s \neg\varphi_0$, *there exists a sequence of pShTL formula* $\varphi_1, \varphi_2, \ldots, \varphi_n$ *with proper parameters, such that* $\varphi_0 \preceq_s \varphi_1 \preceq_s \varphi_2, \ldots, \preceq_s \varphi_n \preceq_s \varphi$ *and* $\varphi \preceq_s \varphi_n$, *where* $n \geq 1$.

5. Solutions

5.1. Shapelet generation

The ShTL defined in this paper is based on the shapelets. Since every subsequence of the original time series can be a shapelet, taking all the shapelets into consideration for logic inference is unrealistic and unnecessary. Since shapelet generation is not the main focus of this paper, we use the shapelet generation algorithm in Lines et al. (2012) with small modification, such that the algorithm is suitable for ShTL. In this paper, we also use the best k shapelets to construct the pShTL formula for time series classification. We denote the set of all subsequences of length l to be T_l. The process of extracting the k best shapelets is similar to the algorithm in Lines et al. (2012), but we have made some changes since our concern is how to choose shapelets that will classify the data well. First, we care about how the distribution of the distances of the shapelets is different from the distribution from the other classes. We have redefined the procedures *findDistance* in Algorithm 2 in Lines et al. (2012). Moreover, we calculate the time-varying distance for each time series in Γ with respect to each chosen shapelet at the last step. The distances are measured based on the metric defined in Eq. (1), and the distance between a subsequence S of length l and all the subsequences T_l is

$$d_{i,S} = \min_{R \in T_{i,l}} d(S, R) + \beta \bar{d}(S, T_{i,l}), \tag{6}$$

where $\bar{d}(S, T_{i,l})$ is the average distance between S and all the subsequences in $T_{i,l}$, and β is a discount factor that balance the critical case and the average. We introduce the second term since pShTL not only captures the critical scenario but also cares about the temporal properties of the distances. Moreover, in order to speed up the computation process for distance, we use the efficient distance computation method in Mueen et al. (2011). Then all distances between a candidate shapelet S and all series in Γ will be a set of n distance, i.e.,

$$D_S = \langle d_{1,S}, d_{2,S}, \ldots, d_{n,S} \rangle. \tag{7}$$

With D_S, the quality of a shapelet is measured based on the information gain, which sorts the distance set D_S, then evaluates the information gain on the class values for each possible split value. If there are multiple classes in Γ, the F-statistic of a fixed-effects ANOVA can be used and readers can refer Lines et al. (2012) for more details of the shapelet generation method.

5.2. Logic inference algorithm

In this subsection, we introduce the logic inference algorithm in Algorithm 1. The inputs of the Algorithm 1 are the class label set $\mathcal{C}$, two sets $(\mathcal{D}, \mathcal{U})$, where $\mathcal{D}$ denotes the set of distance series come from the desirable series in Υ^+, and $\mathcal{U}$ denotes the set of distance series come from the undesirable series in Υ^-. Line 1 initializes φ_D with a random formula that has the structure chosen from Ω with random parameters. Then the algorithm calculates the robustness of all the time series in $(\mathcal{D}, \mathcal{U})$ in Line 4. Based on the robustness, Line 5 checks whether the time series are classified correctly with the current formula φ_D. $\mathcal{D}^+$ denotes the series in $\mathcal{D}$ are classified correctly, and $\mathcal{U}^+$ denotes the series in $\mathcal{U}$ are classified correctly, respectively. $\mathcal{D}^-$ and $\mathcal{U}^-$ are defined as versa. For example, if a time series in $\mathcal{D}$ has a positive robustness degree, the series is assigned to set $\mathcal{D}^+$. If the series has negative robustness, it will be assigned to set $\mathcal{D}^-$. We can easily find that *FA* in Eq. (4) leads to $\mathcal{D}^-$ and *MD* leads to $\mathcal{U}^-$. Line 7 checks all the shapelets. Line 8 extends the current formula to get two new formulas $\varphi_{and}(\theta)$ and $\varphi_{or}(\theta)$ with parameter vector θ ($8k$ formulas in total for all, where the number 8 comes from the 4 choices of atomic formulas in Ω and their negation, ϕ_j^i and ϕ_j^i are the atomic formulas for shapelet i). Based on the results in Lemma 2, all formulas can be constructed in this way. Line 9 and Line 10 find the optimal parameters for the newly found formulas. The optimization problems are defined in the following.

Algorithm 1 Logic Inference for Time Series Classification

Require: A set of distance series $(\mathcal{D}, \mathcal{U})$ and their class label set C, parameter space Θ and length limit, M, for φ_D.
Ensure: The ShTL formula φ_D for the desirable class.

1: Initialize φ_D as an atomic pShTL formula defined in Ω with random parameters. Set $count = 0$
2: **repeat**
3: $quality \leftarrow \emptyset$, $count \leftarrow count + 1$,
4: $\rho_i \leftarrow calculateRobust(\varphi_D, \mathcal{D}, \mathcal{U})$,
5: $\mathcal{D}^+, \mathcal{D}^-, \mathcal{U}^+, \mathcal{U}^+ \leftarrow assignLable(\rho_i, C)$,
6: **for** $j = 1$ to 8 **do**
7: **for** $i = 1$ to k **do**
8: $\varphi_{and}(\theta) \leftarrow \varphi_D \wedge \phi_j^i$, $\varphi_{or}(\theta) \leftarrow \varphi_D \vee \phi_j^i$,
9: $q_1, \varphi_{and}(\theta^*) \leftarrow optAnd(\mathcal{D}^+, \mathcal{D}^-, \mathcal{U}^-, \varphi_{and}(\theta))$,
10: $q_2, \varphi_{or}(\theta^*) \leftarrow optOr(\mathcal{D}^-, \mathcal{U}^+, \mathcal{U}^-, \varphi_{or}(\theta))$,
11: $quality.add(< q_1, \varphi_{and}(\theta^*) >, < q_2, \varphi_{or}(\theta^*) >)$,
12: $\varphi_D \leftarrow assessFormula(quality)$,
13: **until** $count > M$ or $q_{1/2} == 0$.

Parameter Optimization: The goal of each optimization problem is to find an optimal parameter vector $\theta^* \in \Theta$, such that $\varphi_D \preceq_s \varphi_{and}(\theta^*)$, $\varphi_D \preceq_s \varphi_{or}(\theta^*)$, and the value for $q_{1/2} = |\mathcal{D}^-| + |\mathcal{U}^-|$ is minimum. Therefore, the optimization problems in Line 8 and Line 9 can be defined as,

$$\theta^* = \text{argmin}(|\mathcal{D}^-| + |\mathcal{U}^-|) \tag{8}$$

Subject to:

$$\forall \mathbf{x} \in \mathcal{D}^+, \mathbf{x} \models_s \varphi_{and/or}(\theta^*); \tag{9a}$$

$$\forall \mathbf{x} \in \mathcal{U}^+, \mathbf{x} \not\models_s \varphi_{and/or}(\theta^*). \tag{9b}$$

According to the semantics of ShTL, we can ignore the constraints in (9a) during the optimization process in Line 10, and ignore the constraints in (9b) during the optimization process in Line 9, since they always hold. We solve the optimization problem defined in Eq. (8) with an active learning algorithm called Gaussian process adaptive confidence bound (GP-ACB) defined in Chen et al. (2020). After the optimal parameters have been found, Line 11 saves the formulas and the obtained values for q_1, q_2, then Line 12 chooses the best formula among the formulas in *quality* and assigns it to φ_D. Based on the Lemmas derived above, Algorithm 1 can lead to the following results.

Theorem 3. *Denote* φ_i *as the formula found in the ith iteration in Line 12 in Algorithm 1, the following statements hold,*

(1) $\varphi_1 \preceq_s \varphi_2, \ldots, \preceq_s \varphi_M$;
(2) *If there exists a pShTL formula* φ^* *with proper parameters that can classify the time series in* $(\mathcal{D}, \mathcal{U})$ *correctly, then with a large enough* M, *we have* $\varphi^* \preceq_s \varphi_M$.

Theorem 3 indicates that, if there exists a formula that can classify the time series, Algorithm 1 can find the formula by searching along the monotonic order. Since the number of time series in $\mathcal{U}^-$ and $\mathcal{D}^-$ are non-increasing when searching along the monotonic order, the miss-classification rate is non-increasing. Note that Theorem 3 assumes that the distance series are classifiable with ShTL formula. But it may be not true in practice. Therefore, in Algorithm 1, we set a length limit M to avoid an indefinitely long formula when the distance series are not classifiable with an ShTL formula.

Remark 3. Assume that the number of time series in Γ is n and the average length of each time series is $\bar{m}$, then the size of the candidate shapelets is $\mathcal{O}(\bar{m}^2 n)$. Checking the quality of one candidate takes $\mathcal{O}(\bar{m}n)$. Hence, the complexity of the shapelet generation Algorithm is $\mathcal{O}(\bar{m}^3 n^2)$. Based on Theorem 1, the increase of the length of φ_D in Algorithm 1 will decrease the size of $\mathcal{U}^-$ and $\mathcal{D}^-$. Then the average length of φ_D will be $n/2$. Assume the size of sampling space for parameter θ is H, then the complexity of Algorithm 1 is $\mathcal{O}(knH)$, where k is the number of shapelets. In this paper, we assume the time series are univariate. But the proposed algorithms can also deal with multidimensional time series, in which case, we need to find shapelets for each dimension. Moreover, we need to calculate the shapelet distance for each dimension, which means the dimension of time series in $\mathcal{U}$ and $\mathcal{D}$ will be increased. Assume the dimension of the signals is N, then the complexity for the shapelet generation algorithm and Algorithm 1 will be $\mathcal{O}(N\bar{m}^3 n^2)$ and $\mathcal{O}(NknH)$, respectively. Moreover, since GP-ACB is used to find the optimal formula, the following theorem from Chen et al. (2020) is applicable to construct the relation between robustness and uncertainties.

Theorem 4 (*Theorem 1 in Chen et al. (2020)*). *If the optimal robustness degree from solving (8) is* $\hat{\kappa}$, *and the robustness degree without noise is* κ, *pick* $\delta \in (0, 1)$ *and set* $\beta_t = 2\log(|\Theta|\pi_t/\delta)$, *where* $\sum_{t\geqslant 1} \pi_t^{-1} = 1$. *If we sample the new parameter point* θ *with the strategy proposed in Eqn. (12) in Chen et al. (2020), then after T steps of sampling, we have* $\mathbb{P}(|\hat{\kappa} - \kappa| < \beta_T^{1/2}\sigma(\theta, T-1))$ *holds with probability* $\geqslant 1 - \delta$.

6. Experiment evaluation

In this section, the proposed method is applied to the fault diagnosis tasks for motor bearings. In order to accurately diagnose the faults, fault features should be contained in the sampled signals. Therefore, we assume that the fault will not disappear within the sampled time interval if it has occurred. Moreover, we also assume we know the fault types among the signals, including the number of fault types. The motor bearing signals provided by Case Western Reserve University (Lou & Loparo, 2004) are used for experimental validation. The vibration signals were collected from the drive end of the motor housing in the test rig. Each bearing was tested under four different loads (0, 1, 2, and 3 hp), and single point faults (dents) were introduced to the bearings with fault diameters of 0.007, 0.014, 0.021 and 0.028 inches separately. An accelerometer is placed near the drive end to collect the vibration signals. In this paper, the collected vibration data under 1797 rpm was used to design data samples and the sampling frequency was 12 kHz. Three bearing conditions' signals are collected, including *outer race fault, inner race fault and ball fault*. Each bearing condition consists of 160 samples, including different fault diameters and different loads, and each sample is a vibration signal containing 2000 data points.

To verify the practical effectiveness of the proposed method, the fault diagnosis accuracies for the three type faults are evaluated. Since the signals were contaminated by noises, we first decompose the signals with wavelet package transform at level 2 and calculate the second spectral moment for one component of the decomposed signals for interpretable fault diagnosis. Then, we construct the labeled set Γ for training and testing purpose. To construct the positive set (the signals should have positive robustness degree with respect to an optimal formal) for the inner fault, 80 pieces of inner fault signals are used, and the negative set (the signals should have positive robustness degree with respect to an optimal formal) comes from the other two conditions' signals (40 signals for each). The labeled sets for outer race fault and rolling element fault are constructed accordingly. To construct the testing set for the inner fault conditions, the positive testing examples are the rest 80 pieces, and the negative test examples come from the other two bearing conditions (40 pieces for each condition that un-used for training). Other testing sets are constructed accordingly. Before we start the logic inference procedure, shapelets are selected by running shapelet generation algorithm, where we select 3 shapelets, and the length range of the shapelet is from 10 to 30, respectively. The number of shapelets and their length ranges are set through some experiments, in which we test many choices and check whether the results are acceptable and the results show 3 shapelets with lengths between 10 and 30 are enough. As shown in Fig. 1(d), the generated shapelets's lengths are 18, 23, and 30, respectively.

Table 1 shows the learned ShTL formals with Algorithm 1 and their performance for fault diagnosis. The formula φ_I indicates that the causes for inner race fault are that always between 0.03 and 0.05 s, the distance between the signals and shapelet 1 is smaller than or equal to 0.17 within every 0.015 s, and eventually between 0.07 and 0.15 s, the distance between the signals and shapelet 3 is always larger than 0.15 within 0.01 s. Fig. 1(e,f) shows the visualization of formula φ_I, in which we can see the formula can classify the red signals (positive set) and greed signals (negative set) correctly. The light blue rectangle region indicates the first term of the formula, where the red signals should reach, and the blue region indicates the second term of formula, where the red signals should avoid. Moreover, the combination of "eventual" (**F**) and "always" (**G**) operators allows the regions moving along the time axis, which illustrates the expressiveness of the formula and equips the formula with shift-invariance property. Moreover, the average variances of the original signals, the shapelet distance for shapelet 1 and 3 are 0.0175, 0.0022, and 0.0017, respectively. Compared with the original signals, the variance of the shapelet distances are smaller, which means ShTL is more robust than STL to noise. The other two formulas can be interpreted in the same way and is omitted here due to page limit. The fault diagnosis accuracy shows the proposed method can obtain good performance since the error rate is smaller than 5%. Fig. 1(b,c) shows the spectrogram of the signal that generates shapelet 1 and 3, respectively. The spectrograms indicate that shapelet 1 reveals the high-frequency component of the signal and shapelet 3 reveals the low-frequency component of the signal. When the shapelet's spectrogram is distributed in a low-frequency region, the distance between the shapelet and low-frequency signal will be small. In contrast, when the shapelet's spectrogram is distributed in the high-frequency region, the distance between the shapelet and the high-frequency signal will be small. Moreover, since a high-frequency signal usually leads to large variance, it also has large shapelet distance components. The visualization of formula φ_I in Fig. 1(e,f) indicates the red signals have more high-frequency components, while the

Table 1
Interpretation formulas for the real experimental vibration signals for inner race, outer race and rolling element faults.

Fault type	Interpretation formula	Robustness		Accuracy rate	
–	–	Training	Testing	Training	Testing
Inner race (φ_I)	$\mathbf{G}_{[0.03,0.05]}(\mathbf{F}_{[0,0.015]}(f(s_1,\mathbf{x}) \le 0.17)) \wedge \mathbf{F}_{[0.07,0.15]}(\mathbf{G}_{[0,0.01]}(\neg(f(s_3,\mathbf{x}) \le 0.15)))$	0.014	0.009	1.000	1.000
Outer race (φ_O)	$\mathbf{G}_{[0.02,0.1]}(\mathbf{F}_{[0,0.03]}(f(s_1,\mathbf{x}) \le 0.12))$	0.004	0.021	1.000	1.000
Ball (φ_B)	$(\mathbf{F}_{[0.06,0.94]}(\neg(f(s_1,\mathbf{x}) \le 0.26)) \wedge \mathbf{G}_{[0.097,0.13]}(\neg(f(s_2,\mathbf{x}) \le 0.13))$	0.005	−0.018	1.000	0.975

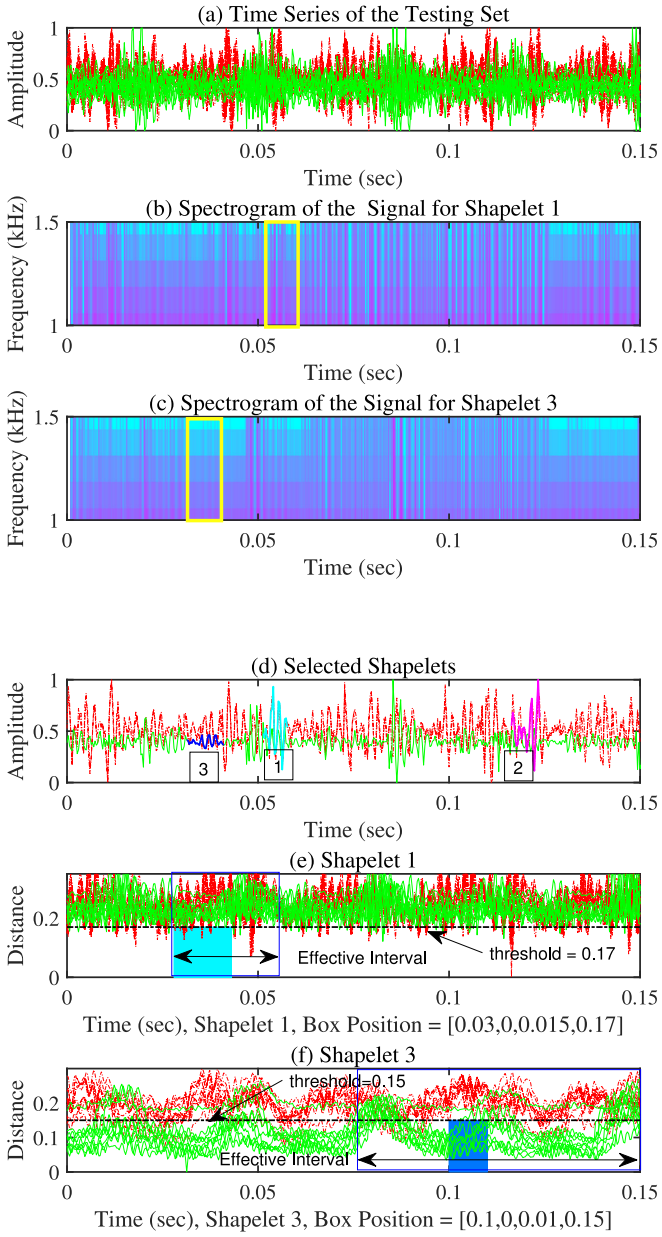

Fig. 1. (a) Some selected time series among the testing set; (b) The spectrogram of the signal that generates shapelet 1; (c) The spectrogram of the signal that generates shapelet 3; (d) the selected 3 shapelets with different colors; (e) The shapelet distance between shapelet 1 and the signals in inner fault's testing set and the formula (φ_I first term) defined region; (f) The shapelet distance between shapelet 3 and the signals in the inner fault's testing set and the formula (φ_I second term) defined region. (For interpretation of the references to color in this figure legend, the reader is referred to the web version of this article.)

green signals have more low-frequency components. Based on the fault mechanism of rolling-element bearing in Chen et al. (2022), the inner race fault has a larger ballpass frequency than other conditions, thus the inner race fault signals have more high-frequency components. Therefore, the interpretation of the formula is in line with the fault mechanism.

An ShTL formula maps a set of observed phenomena and their temporal relationships to a fault event. The phenomena reveal physical processes among the systems, which can be understood by human users with some background knowledge, thus the formula is interpretable. When we monitor the condition for a safety-critical system, for example, the nuclear power plant, interpretable fault diagnosis results provided by ShTL formulas are critically important for the users. If the results are not interpretable, the users will not trust the decision made by the fault diagnosis algorithm or it will take a long time for the users to trust the decision and take necessary preventive actions. The delay caused by trust issues may lead to heavy losses. Moreover, the shapelet reveals which behaviors of the system affect the fault diagnosis decision, thus it provides a more detailed explanation for the decision process and helps the users take a quick action to control the fault. For example, since shapelet 1, which has high-frequency property, affects the fault diagnosis decision in the bearing fault diagnosis experiment, we can add lubricating oil to reduce the high-frequency component to control the fault.

Table 2 compares the proposed method with methods in Chen et al. (2020) and Lines et al. (2012), which shows the average faults diagnosis results for the experimental data among 10 tails. In Lines et al. (2012), the shapelets are extracted and then support vector machine (SVM) is used to classify the faults and in Chen et al. (2020) the frequency temporal logic (FTL) is used to describe the faults, where the formulas are learned with deep neural network. The results show the our method has comparable fault diagnosis accuracy, but has worse efficiency. However, the proposed method has better interpretation abilities, since classifying the faults with SVM in Lines et al. (2012) cannot reveal how the shapelets affect the decision process, and without using shapelet in Chen et al. (2020), the users cannot know which component of the signals are related to fault diagnosis results.

Table 3 shows the number of signals in $\mathcal{D}^+$, $\mathcal{D}^-$, $\mathcal{U}^+$ and $\mathcal{U}^-$ with different formula lengths. The results show that when the formula length increases, the number of signals in $\mathcal{D}^+$ and $\mathcal{U}^+$ will increase, while the number of signals in $\mathcal{D}^-$ and $\mathcal{U}^-$ will decrease, indicating that more signals will be classified correctly with the increase of formula length. This result confirms that Algorithm 1 increases the formula length along the partial order direction. Moreover, Fig. 1(e,f) show the effective intervals of the two sub-formulas of φ_I. It is clear that the two effective intervals do not have any intersection region along the time axis. Based on the definition of parallel formulas in Definition 4, the two sub-formulas are parallel.

We also investigate the noisy resistance properties of the ShTL formula in bearing fault diagnosis with simulated signals. In the first simulation setting, we investigate the performance of the proposed method with different levels of noise by changing the signal-to-noise ratio (SNR). The training set, and testing set are constructed in the same way as the first experiment, but the signals are collected with the fault model defined in Chen et al. (2022). In this experiment, we only change the SNR and fixed the rotational speed. The average error rates of 10 trails are shown in Table 4. The results show that the proposed method can obtain good performance even though the SNR is −15 dB,

Table 2
Diagnosis accuracies of different methods.

Fault type	Accuracy/Time (s)		
–	ShTL	Shapelet (Lines et al., 2012)	FTL (Chen et al., 2020)
Inner race	1.000/1043	1.000/866	1.000/415
Outer race	1.000/1003	1.000/875	0.950/428
Ball	0.975/1013	1.000/879	1.000/435

Table 3
Illustration of exploration via partial order direction.

Fault type	# $\mathcal{D}^+$	# $\mathcal{D}^-$	# $\mathcal{U}^+$	# $\mathcal{U}^-$
Formula length	1/2	1/2	1/2	1/2
Inner race (φ_I)	65/80	15/0	53/80	27/0
Outer race (φ_O)	80/–	0/–	80/–	0/–
Ball (φ_B)	47/78	33/2	67/80	13/0

Table 4
Results for different signal to noise ratio.

SNR (dB)	Error rate (%)				
	−20	−15	−10	0	10
Inner race (φ_I)	11.50	3.75	0.00	0.00	0.00
Outer race (φ_O)	12.25	1.50	0.00	0.00	0.00
Ball (φ_B)	12.00	4.50	0.00	0.00	0.00

indicating the method is robust to noise. The reason for this is that the shapelet distance is the average distance between the shapelet and the signal, which acts as a filter applied to the vibration signals. Table 5 shows the formulas obtained with $SNR = -10$ db. We can see that the structure of the interpretation is the same with formulas in Table 1, but they have different parameters for the formulas. This is reasonable since only the structure of the formula shows the observed physical phenomena and their temporal relationship under the fault condition. These phenomena and relationships are related to the fault mechanism, which should be unchanged.

7. Conclusions

This paper introduces a formal language that classifies time series for fault diagnose. An algorithm has been developed to infer the logic formula, which can be used to describe the properties of the shapelets and diagnosis the faults with performance guarantees. Experiments on rolling element bearing datasets indicate the proposed method has comparable fault diagnosis accuracy but has better performance in fault interpretation. However, the proposed method takes more time to find the classifier. Therefore, further studies should address the computational complexity of the proposed method and apply the method to industrial fields, such as real-time motion classification and electroencephalogram (EEG) classification.

Appendix

A.1. Proof of Lemma 1

Proof. (1) We have $\varphi_3 = F_{[0,c)}\varphi_1 = F_{[0,c)}F_{[0,a)}\varphi$. φ_3 requires that φ is eventually true within $[0, a+c)$. Since $\varphi_1 = F_{[0,a')}\varphi$, which requires φ is eventually true within $[0, a')$. Here we use a' for φ_1 to differ the parameters notations. The parameter for φ_1 is a' and the parameters for φ_3 are a and b. For every valuation of the parameters for φ_3, we can always find a valuation for φ_1 that is equal to $a+c$, such that $\mathcal{L}^e(\varphi_1) = \mathcal{L}^e(\varphi_3)$. Condition (1) holds.

(2) We have $\varphi_3 = G_{[0,c)}\varphi_2 = G_{[0,c)}G_{[0,b)}\varphi$. φ_3 requires that φ is always true within $[0, b+c)$. Since $\varphi_2 = G_{[0,b')}\varphi$, which requires φ is always true within $[0, b')$. The parameter for φ_2 is b' and the parameters for φ_3 are c and b. For every valuation of the parameters for φ_3, there exists a valuation for φ_2 that is equal to $b+c$, such that $\mathcal{L}^e(\varphi_2) = \mathcal{L}^e(\varphi_3)$. Condition (2) holds.

(3) We have $\varphi_3 = G_{[0,c)}\varphi_1 = G_{[0,c)}F_{[0,a)}\varphi$. φ_3 requires that φ is eventually true within $[t, t+a)$ for any $t \in [0, c)$. Since $\varphi_1 = F_{[0,a')}\varphi$, which requires φ is eventually true within $[0, a')$. For any time series that satisfies φ_3, it must satisfy φ_1 at some time starting within $[0, c)$, namely $\mathcal{L}^e(\varphi_3) \subseteq \mathcal{L}^e(\varphi_1)$. Condition (3) holds.

(4) We have $\varphi_3 = F_{[0,c)}\varphi_2 = F_{[0,c)}G_{[0,b)}\varphi$. φ_3 requires that φ is always true within $[t, t+b)$ for any $t \in [0, c)$. Since $\varphi_2 = G_{[0,b')}\varphi$, which requires φ is always true within $[0, b')$. For any time series that satisfies φ_1, it must satisfy φ_3 at some time starting within $[0, c)$, namely $\mathcal{L}^e(\varphi_2) \subseteq \mathcal{L}^e(\varphi_3)$. Condition (4) holds. □

A.2. Proof of Lemma 2

Proof. Based on the syntax of ShTL and the results in Lemma 1, the following statements hold: (1) if $\mathbf{x} \in \mathcal{L}^e(FF\varphi)$, then $\mathbf{x} \in \mathcal{L}^e(F\varphi)$; (2) if $\mathbf{x} \in \mathcal{L}^e(GG\varphi)$, then $\mathbf{x} \in \mathcal{L}^e(G\varphi)$; (3) if $\mathbf{x} \in \mathcal{L}^e(GF\varphi)$, then $\mathbf{x} \in \mathcal{L}^e(F\varphi)$; (4) if $\mathbf{x} \in \mathcal{L}^e(FGFG\varphi)$, then $\mathbf{x} \in \mathcal{L}^e(FG\varphi)$; (5) if $\mathbf{x} \in \mathcal{L}^e(GFGF\varphi)$, then $\mathbf{x} \in \mathcal{L}^e(GF\varphi)$.

Here we omit the parameters for operators F, G for simplicity. Therefore, for all $\mathbf{x}$ that satisfies an ShTL formula, it can satisfy a formula defined by the following syntax,

$$\varphi = \mu|\neg\varphi|F\mu|G\mu|FG\mu|GF\mu|\varphi_1 \wedge \varphi_2|\varphi_1 \vee \varphi_2, \tag{10}$$

where μ is the predicate in Eq. (2), which is ϕ_0 in Ω. Therefore, Lemma 2 has been proven. □

A.3. Proof of Theorem 1

Proof. When φ has only one predicate, the theorem is obviously true. When φ has more than one predicate, φ can be written as: (i) $\varphi = \varphi_n = \varphi_1 \wedge \varphi_{n-1}$ or (ii) $\varphi = \varphi_n = \varphi_1 \vee \varphi_{n-1}$, where φ_1 has only one predicate. Assume $\mathcal{D}_i^+$ is the set for desirable series that have been classified correctly with φ_i, and $\mathcal{D}_i^-$ is the set for desirable series that have been classified incorrectly with φ_i. $\mathcal{U}_i^+$, $\mathcal{U}_i^-$ are for the undesirable series.

For case (i), If φ_{n-1} classifies the series correctly, obviously $\varphi_{n-1} \preceq_s \varphi_n$, else φ_1 decreases the number of time series in $\mathcal{U}_{n-1}^-$. Since for any time series $\mathbf{x}$, it must satisfy φ_{n-1} or do not satisfy φ_{n-1}. Therefore, there exists φ_1, such that $\neg\varphi_1 \parallel_{\mathcal{U}_{n-1}^-} \neg\varphi_{n-1}$, where $\neg\varphi_1$ is the negation of φ_1, and $\forall \mathbf{x} \in \mathcal{D}_{n-1}^+ \Rightarrow \mathbf{x} \models_s \varphi_1 \wedge \varphi_{n-1}$, therefore, $\varphi_{n-1} \preceq_s \varphi_n$.

For case (ii), If φ_{n-1} classifies the series correctly, obviously $\varphi_{n-1} \preceq_s \varphi_n$, else φ_1 decrease the number of time series in $\mathcal{D}_{n-1}^-$. Since for any time series $\mathbf{x}$, it must satisfy φ_{n-1} or not satisfy φ_{n-1}. Therefore, there exists φ_1, such that $\varphi_1 \parallel_{\mathcal{D}_{n-1}^-} \varphi_{2n-1}$, and $\forall \mathbf{x} \in \mathcal{U}_{n-1}^+ \Rightarrow \mathbf{x} \models_s \varphi_1 \vee \varphi_{n-1}$, therefore, $\varphi_{n-1} \preceq_s \varphi_n$.

Since the time series classified by φ_1 and φ_{n-1} have different effective interval, there exists $\varphi_{n-2} \preceq_s \varphi_{n-1}$ based on the above derivations. Therefore, there exists a sequence of pShTL formulas, such that $\varphi_1 \preceq_s \varphi_2 \preceq_s \cdots \preceq_s \varphi_n \preceq_s \varphi$. When n is large enough, we have $\mathcal{D}_n^- = \emptyset$ and $\mathcal{U}_n^- = \emptyset$, i.e., $\varphi \preceq_s \varphi_n$. Moreover, the number of predicates satisfies the following property,

$$|\varphi_n| - |\varphi_i| = n - i, \tag{11}$$

where $n \geq i \geq 1$. Theorem 1 has been proven. □

Table 5
Interpretation formulas for the simulated signals with $SNR = -10$ db.

Fault type	Interpretation formula
Inner race	$\mathbf{G}_{[0.03,0.07]}(\mathbf{F}_{[0,0.01]}(f(s_2,\mathbf{x}) \le 0.21)) \wedge \mathbf{F}_{[0.09,0.15]}(\mathbf{G}_{[0,0.01]}(\neg(f(s_3,\mathbf{x}) \le 0.16)))$
Outer race	$\mathbf{G}_{[0.04,0.12]}(\mathbf{F}_{[0,0.04]}(f(s_2,\mathbf{x}) \le 0.16))$
Ball	$(\mathbf{F}_{[0.02,0.05]}(\neg(f(s_1,\mathbf{x}) \le 0.16)) \wedge \mathbf{G}_{[0.07,0.15]}(\neg(f(s_2,\mathbf{x}) \le 0.12))$

A.4. Proof of Theorem 2

Proof. Based on the assumption, we have $\forall \mathbf{x} \in \Upsilon^+ \Rightarrow \mathbf{x} \models_s \varphi_0$. Denote $\mathcal{U}^+ \subseteq \Upsilon^-, \mathcal{U}^- \subseteq \Upsilon^-$, where $\forall \mathbf{x} \in \mathcal{U}^+ \Rightarrow \mathbf{x} \models_s \neg\varphi_0$ and $\forall \mathbf{x} \in \mathcal{U}^- \Rightarrow \mathbf{x} \models_s \varphi_0$. To prove the theorem, we first prove that one of the following statements,

(1) there exists a *pShTL* formula φ_{and} with proper parameters that can classify time series in $\mathcal{D}^+$ and $\mathcal{U}^-$, such that $\varphi_0 \wedge \varphi_{and}$ can classify Υ^+ and Υ^-;
(2) there exists a *pShTL* formula φ_{or} with proper parameters that can classify time series in $\mathcal{D}^-$ and $\mathcal{U}^-$, such that $\varphi_0 \vee \varphi_{and}$ can classify Υ^+ and Υ^-.

Since the time series in Υ^+ and Υ^- are classifiable with an ShTL formula, the time series in $\mathcal{D}^+$ and $\mathcal{U}^-$, and $\mathcal{D}^-$ and $\mathcal{U}^-$ are classifiable too. Therefore, statements (1) and (2) hold. Based on Theorem 1, there exists a sequence of pShTL formula $\varphi_1^a, \varphi_2^a, \cdots, \varphi_n^a$ with proper parameters, such that $\varphi_1^a \preceq_s \varphi_2^a, \ldots, \preceq_s \varphi_n^a \preceq_s \varphi_{and}$ for statement (1). Similarly, there exists a sequence of pShTL formula $\varphi_1^o, \varphi_2^o, \cdots, \varphi_n^o$ with proper parameters, such that $\varphi_1^o \preceq_s \varphi_2^o, \ldots, \preceq_s \varphi_n^o \preceq_s \varphi_{or}$ for statement (2). Denote $\varphi_i = \varphi_i^a \wedge \varphi_0$ or $\varphi_i = \varphi_i^o \wedge \varphi_0$ for $i = 1, 2, \ldots, n$. When n is large enough, we have $\mathcal{D}_n^- = \emptyset$ and $\mathcal{U}_n^- = \emptyset$, i.e., $\varphi \preceq_s \varphi_n^{a/o}$, then Theorem 2 has been proven. □

A.5. Proof of Theorem 3

Proof. Proof for item (1): Based on the definition of monotonic order and the constraints in Eqs. (9a) and (9b), statement (1) holds.

Proof for item (2): When we solve the optimization problem in Line 8 of Algorithm 1, we have $\forall \mathbf{x} \in \mathcal{D}^+ \Rightarrow \mathbf{x} \models \varphi_j$. Since the time series in $\mathcal{U}^-$ and $\mathcal{D}^-$ are classifiable, φ_j will decrease the value for q_1. Based on Theorem 2, if we ignore $\mathcal{D}^-$, Algorithm 1 will eventually decrease $\mathcal{U}^-$ to zero. Similarly, when we solve the optimization problem in Line 9 of Algorithm 1, we have $\forall \mathbf{x} \in \mathcal{U}^+ \Rightarrow \mathbf{x} \models \neg\varphi_j$. Since the time series in $\mathcal{U}^-$ and $\mathcal{D}^-$ are classifiable, φ_j will decrease the value for q_2. Based on Corollary 1, if we ignore $\mathcal{U}^-$, the Algorithm 1 will eventually decrease $\mathcal{D}^-$ to zero. Theorem 3 has been proven. □

References

Baldán, F. J., & Benítez, J. M. (2019). Distributed fastshapelet transform: a big data time series classification algorithm. *Information Sciences*, *496*, 451–463.

Bergé, J., Massey, R., Baghi, Q., & Touboul, P. (2019). Exponential shapelets: Basis functions for data analysis of isolated features. *Monthly Notices of the Royal Astronomical Society*, *486*(1), 544–559.

Chen, G., Liu, M., & Chen, J. (2020). Frequency-temporal-logic-based bearing fault diagnosis and fault interpretation using Bayesian optimization with Bayesian neural networks. *Mechanical Systems and Signal Processing*, *145*, Article 106951.

Chen, G., Wei, P., Jiang, H., & Liu, M. (2022). Formal language generation for fault diagnosis with spectral logic via adversarial training. *IEEE Transactions on Industrial Informatics*, *18*(1), 119–129.

Deshmukh, J. V., Donzé, A., Ghosh, S., Jin, X., Juniwal, G., & Seshia, S. A. (2017). Robust online monitoring of signal temporal logic. *Formal Methods in System Design*, *51*(1), 5–30.

Keogh, E., & Kasetty, S. (2003). On the need for time series data mining benchmarks: A survey and empirical demonstration. *Data Mining and Knowledge Discovery*, *7*(4), 349–371.

Lines, J., Davis, L. M., Hills, J., & Bagnall, A. (2012). A shapelet transform for time series classification. In *Proceedings of the 18th ACM SIGKDD international conference on knowledge discovery and data mining* (pp. 289–297). ACM.

Lou, X., & Loparo, K. A. (2004). Bearing fault diagnosis based on wavelet transform and fuzzy inference. *Mechanical Systems and Signal Processing*, *18*(5), 1077–1095.

Mueen, A., Keogh, E., & Young, N. (2011). Logical-shapelets: An expressive primitive for time series classification. In *Proceedings of the 17th ACM SIGKDD international conference on knowledge discovery and data mining* (pp. 1154–1162). ACM.

Yang, Z.-b., Zhang, J.-p., Zhao, Z.-b., Zhai, Z., & Chen, X.-f. (2020). Interpreting network knowledge with attention mechanism for bearing fault diagnosis. *Applied Soft Computing*, *97*, Article 106829.

Ye, L., & Keogh, E. (2009). Time series shapelets: A new primitive for data mining. In *Proceedings of the 15th ACM SIGKDD international conference on knowledge discovery and data mining* (pp. 947–956). ACM.

Zhao, B., Cheng, C., Tu, G., Peng, Z., He, Q., & Meng, G. (2021). An interpretable denoising layer for neural networks based on reproducing kernel Hilbert space and its application in machine fault diagnosis. *Chinese Journal of Mechanical Engineering*, *34*(1), 1–11.

Gang Chen received the bachelor's and master's degrees in mechanical engineering from Shanghai Jiao Tong University, Shanghai, China, in 2012 and 2015, respectively and his Ph.D. degree in mechanical and aerospace engineering from the University of California, Davis, Davis, CA, in 2020. He was a research fellow with the School of Electrical and Electronic Engineering, Nanyang Technological University, Singapore from 2020 to 2021. He is currently an Assistant Professor at the Shien-Ming Wu School of Intelligent Engineering, South China University of Technology, China. His research interests include machine learning, formal methods, control, signal processing and fault diagnosis.

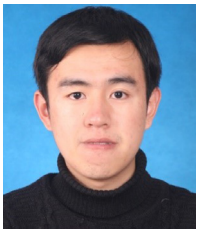

Yu Lu received his B.S. degree in automation from Nanjing University of Science & Technology, Nanjing, China in 2015, and the Ph.D. degree in control science and engineering from Shanghai Jiao Tong University, Shanghai, China in 2020. He was a research fellow with the School of Electrical and Electronic Engineering, Nanyang Technological University, Singapore from 2020 to 2021. He is currently an associate professor with the School of Energy and Power Engineering, Nanjing University of Science & Technology. His research interests include formation cooperation of autonomous systems (e.g., UAVs, ASVs), robust adaptive control, fault-tolerant control and prescribed performance control.

Dr Rong Su obtained his Bachelor of Engineering degree from the University of Science and Technology of China in 1997, and Master of Applied Science degree and Ph.D. degree from the University of Toronto in 2000 and 2004, respectively. He was affiliated with the University of Waterloo and Technical University of Eindhoven before he joined Nanyang Technological University in 2010. Dr Su's research interests include multi-agent systems, discrete-event system theory, model-based fault diagnosis, cyber security analysis and synthesis, control and optimization of complex networks with applications in flexible manufacturing, intelligent transportation and green buildings. In the aforementioned areas he has more than 230 journal and conference publications, 1 monograph, 9 granted/filed patents. Dr Su is a senior member of IEEE, and an associate editor for Automatica (IFAC), Journal of Discrete Event Dynamic Systems: Theory and Applications, and Journal of Control and Decision. He was the Chair of the Technical Committee on Smart Cities in the IEEE Control Systems Society in 2016-2019, and currently a co-chair of IEEE RAS TC on Automation in Logistics. Dr Su is the recipient of 2021 Hsue-shen Tsien Paper Award from IEEE/CAA Journal of Automatica Sinica, and an IEEE Distinguished Lecturer for IEEE RAS.